Contribution from the Department of Chemistry and Molecular Structure Center, Indiana University, Bloomington, Indiana 47405, and Lawrence Livermore National Laboratory, Livermore, California 94550

Preparation and Properties of Mononuclear Vanadium Thiolates: Structural Characterization of the $[V(SBu^t)_4]^{0,-}$ Pair and C-S Bond Cleavage in $V(SBu^t)_4$ in the Gas Phase

Dwight D. Heinrich,[1a] Kirsten Folting,[1a] John C. Huffman,[1a] John G. Reynolds,*[,1b] and George Christou*[,1a]

Received May 7, 1990

The synthesis and properties of mononuclear vanadium complexes with Bu^tS^- ligation are reported. Treatment of $VCl_3(THF)_3$ with $NaSBu^t$ and Bu^tSSBu^t in MeCN leads to high-yield isolation of $V(SBu^t)_4$ (**1**). In contrast, treatment of $VCl_3(THF)_3$ with $NaSBu^t$ and 2,2'-bipyridine (bpy) leads to the V^{III} salt $[V(SBu^t)_2(bpy)_2][V(SBu^t)_4]$ (**2**). Complex **1** crystallizes in space group $P\bar{4}2_1c$ with (at −158 °C) $a = b = 11.034$ (12) Å, $c = 9.253$ (9) Å, and $Z = 2$. Complex **2** crystallizes in space group $P2_1/n$ with (at −142 °C) $a = 21.309$ (9) Å, $b = 15.592$ (6) Å, $c = 17.151$ (7) Å, and $Z = 4$. The structures of **1** and **2** were solved by using 483 ($F > 3.0\sigma(F)$) and 2102 ($F > 2.0\sigma(F)$) unique reflections in the range $6° \le 2\theta \le 45°$ and refined to values of R (R_w) of 3.96 (4.00) and 8.54% (7.69%), respectively. The structure of **1** consists of a mononuclear four-coordinate $V(SBu^t)_4$ unit with imposed $\bar{4}$ (S_4) symmetry, corresponding to a slight flattening from T_d symmetry. The V-S distances are 2.2184 (24) Å. Complex **2** contains an anion that is the one-electron-reduced version of **1**; there is no imposed symmetry, but the geometry can be again described as distorted tetrahedral. The V-S bonds (2.280 (7)-2.309 (7) Å) are slightly longer than those in **1**, as expected for the lower oxidation state. The cation geometry of **2** is distorted octahedral with two chelating bpy groups and two Bu^tS^- ligands in cis positions. Complex **1** was investigated by cyclic voltammetry (CV) in CH_2Cl_2; it was found to undergo a reversible one-electron reduction at −0.68 V vs SCE and an irreversible one-electron oxidation at +0.81 V. The EPR spectrum of **1** in toluene solution at room temperature shows a typical eight-line hyperfine-structured signal with $g_{iso} = 1.970$ and $A_{iso} = 55$ G. At 163 K in a toluene glass, an axially symmetric spectrum is obtained with $g_\parallel = 1.961$, $g_\perp = 1.975$, $A_\parallel = 108$ G, and $A_\perp = 28$ G; these parameters are compared to those for $V(OBu^t)_4$ and differences shown to be as expected for the O vs S substitution. The electron ionization mass spectral (EIMS) behavior of **1** has been investigated and its fragmentation pattern elucidated. The major fragmentation modes involve sequential loss of C_4H_9 by C-S bond cleavage to yield $[V(SBu^t)_{4-x}S_x]^+$ ($x = 0$-4) ions and S atom loss leading to ions of general formulation $[V(SC_4H_9)_xS_y]^+$ ($x = 1, 2$; $y = 1, 2$) and $[VS_x]^+$ ($x = 0$-3). No evidence for one-step loss of an entire SC_4H_9 fragment is observed. The relevance of these results to several catalytic processes in the petroleum industry are described, including the mechanism by which V_2S_3 is formed during upgrading of heavy crudes containing vanadyl impurities and the use of colloidal VS_x particles as hydrodesulfurization catalysts in slurry-type processes.

One of the driving forces behind our current interest in vanadium-sulfur chemistry is the relevance of this area to certain processes in the petroleum industry, specifically crude oil refining. Crude oils have varying levels of organically bound sulfur (thiophenes, thiols, and disulfides)[2] and metals (principally V, Ni, and Fe).[3] In the conversion of crude oils to transportation fuels, these elements are typically considered impurities and must be removed for upgrading.[4] A lot of technology has been developed around the large-scale removal of S[5] and, more recently, in dealing with the high metal content associated with heavy crude oils.[6] Many S-removal processes utilize heterogeneous catalysts that have active chemical sites sensitive to even low-level contamination by metal-containing compounds. These oil-soluble metal species generally end up deposited on the catalyst and can cause the demise of the activity of the catalyst pore.[7] For heavy crude oils, V and Ni are generally the most deleterious metal components. The binding of vanadium in crude oils is not unequivocally known but is generally recognized as occurring in two forms, the metallopetroporphyrins and metallo-non-porphyrins.[8] The metallopetroporphyrins consist of a porphyrin ring with the four nitrogens binding a vanadyl unit and alkyl substituents on the outside of the ring.[9] The nature of the non-porphyrins is not nearly so well-defined but is thought to consist of the vanadyl ion bound by various ligands to form a square-pyramidal system.[10] These ligand structures are thought to provide combinations of S, N, and/or O in the basal plane of the first coordination sphere. Although some studies have been carried out, the molecular mechanisms for the deposition of the metals on the catalyst surface have not been completely elucidated.[11-14] However, it is known that the deposited forms of the metals are the sulfides. Exactly what are the identities of the M/S intermediates in this conversion of crude oil impurities into metal sulfides is currently unclear.

Our development of the coordination geometry of V in a completely or partially sulfur environment has been designed to provide a solid foundation for attempting to redress this lack of detailed knowledge. In recent reports, we have described the preparation and properties of a variety of discrete V/S/RS^- complexes, of various nuclearities and oxidation levels, with R = Ph or bidentate thiolates.[15-20] More recently, we have employed Bu^tS^- as a ligand and have prepared the four-coordinate species $V(SBu^t)_4^{z-}$ as both

(1) (a) Indiana University. (b) Lawrence Livermore National Laboratory.
(2) (a) Orr, W. L. *Oil Sand and Oil Shale Chemistry*; Verlag Chemie: Weinheim, Germany, 1978; p 223. (b) Cyr, T. D.; Payzant, J. D.; Montgomery, D. S.; Strausz, O. P. *Org. Geochem.* **1986**, *9*, 139. (c) Nishioka, M. *Energy Fuels* **1988**, *2*, 214.
(3) Reynolds, J. G.; Biggs, W. R. *Acc. Chem. Res.* **1988**, *21*, 319.
(4) Branthaver, J. F. *ACS Symp. Ser.* **1987**, *No. 344*, 188.
(5) Ranney, M. W. *Desulfurization of Petroleum*; Noyes Data: Park Ridge, NJ, 1975.
(6) Speight, J. G. *The Chemistry and Technology of Petroleum*; Marcel Dekker: New York, 1980; Vol. 3.
(7) Tamm, P. W.; Harnsberger, H. F.; Bridge, A. G. *Ind. Eng. Chem. Process Des. Dev.* **1981**, *20*, 262.
(8) Yen, T. F. In *The Role of Trace Metals in Petroleum*; Ann Arbor Science: Ann Arbor, MI, 1975; Chapter 1.
(9) Psundararaman, P. *Anal. Chem.* **1986**, *57*, 2204.
(10) Reynolds, J. G.; Gallegos, E. J.; Fish, R. H.; Komlenic, J. J. *Energy Fuels* **1987**, *1*, 36.
(11) (a) Silbernagel, B. G.; Mohan, R. R.; Singhal, G. H. *ACS Symp. Ser.* **1984**, *No. 248*, 91. (b) Silbernagel, B. G. *J. Catal.* **1979**, *56*, 315.
(12) Asaoka, S.; Nakata, S.; Takeuchi, C. *ACS Symp. Ser.* **1987**, *No. 344*, 275.
(13) Rosa-Brussin, M.; Moranta, D. *Appl. Catal.* **1984**, *11*, 85.
(14) Mitchell, P. C. H.; Scott, C. E.; Bonnelle, J.-P.; Grimblot, J. G. *J. Chem. Soc., Faraday Trans. 1* **1985**, *81*, 1047.
(15) (a) Money, J. K.; Huffman, J. C.; Christou, G. *Inorg. Chem.* **1985**, *24*, 3297. (b) Money, J. K.; Folting, K.; Huffman, J. C.; Collison, D.; Temperley, J.; Mabbs, F. E.; Christou, G. *Inorg. Chem.* **1986**, *25*, 4583.
(16) Money, J. K.; Nicholson, J. R.; Huffman, J. C.; Christou, G. *Inorg. Chem.* **1986**, *25*, 4072.
(17) Money, J. K.; Huffman, J. C.; Christou, G. *J. Am. Chem. Soc.* **1987**, *109*, 2210.
(18) Money, J. K.; Folting, K.; Huffman, J. C.; Christou, G. *Inorg. Chem.* **1987**, *26*, 944.
(19) Money, J. K.; Huffman, J. C.; Christou, G. *Inorg. Chem.* **1988**, *27*, 507.
(20) Christou, G.; Heinrich, D. D.; Money, J. K.; Rambo, J. R.; Huffman, J. C.; Folting, K. *Polyhedron* **1989**, *8*, 1723.

0020-1669/91/1330-0300$02.50/0

Table I. Crystallographic Data for Complexes **1** and **2**

param	1	2
space group	$P\bar{4}2_1c$	$P2_1/n$
a, Å	11.034 (12)	21.309 (9)
b, Å	11.034 (12)	15.592 (6)
c, Å	9.253 (9)	17.151 (7)
β, deg	90	94.00 (2)
Z	2	4
V, Å^3	1126.67	5684.72
formula	$C_{16}H_{36}S_4V$	$C_{44}H_{70}N_4S_6V_2$[a]
M_r	407.64	1035.48
ρ_{calc}, g cm^{-3}	1.202	1.210
μ, cm^{-1}	7.771	5.632
T, °C	−158	−142
λ, Å	0.710 69	0.710 69
range, deg	$6 \le 2\theta \le 45$	$6 \le 2\theta \le 40$
no. of obsd data	483	2102
R (R_w), %	3.96 (4.00)	8.54 (7.69)

[a] Excluding disordered solvate atoms.

the neutral ($z = 0$; V^{IV}) and monoanionic ($z = 1$; V^{III}) forms. We considered the neutral form to be a good candidate for a mass spectral investigation of its fragmentation pattern, believing the obtained results might be of some utility as a model system for some of the high-energy reactions occurring during hydrodemetalation/hydrodesulfurization petroleum processes. The combined results of this work are described herein.

Experimental Section

Syntheses. All manipulations were carried out under anaerobic conditions employing standard Schlenk techniques and freshly distilled and degassed solvents. 2,2′-bipyridine (bpy) and Bu^{t}SSBu^t were used as received. $VCl_3(THF)_3$ was prepared as described in the literature.[21] NaSBu^t was prepared by adding sodium metal to a THF solution containing a slight excess of Bu^{t}SH; the resulting white solid was collected by filtration, washed with THF, and dried under vacuum.

V(SBu^t)$_4$ (1). $VCl_3(THF)_3$ (0.72 g, 2.0 mmol) and NaSBu^t (0.67 g, 6.0 mmol) were dissolved in MeCN (50 cm^3) to give a deep red solution, followed by addition of Bu^{t}SSBu^t (0.20 cm^3, 1.03 mmol) by syringe. After 1 h, MeCN was removed under vacuum and the residue extracted with Et_2O or hexanes. The dark red solution was filtered and the product isolated as a red-black powder by removal of the solvent under vacuum. The yield from multiple preparations was 40–65%. Anal. Calcd for $C_{16}H_{36}S_4V$: C, 47.14; H, 8.90; S, 31.46; V, 12.50. Found: C, 47.44; H, 8.91; S, 30.85; V, 12.95. Crystals suitable for crystallography were obtained by storing a concentrated MeCN solution in a freezer overnight.

[V(SBu^t)$_2$(bpy)$_2$][V(SBu^t)$_4$] (2). A slurry of $VCl_3(THF)_3$ (0.72 g, 2.0 mmol), NaSBu^t (0.70 g, 6.2 mmol), and bpy (0.32 g, 2.0 mmol) in THF (60 cm^3) was stirred for 1.5 h and the resulting deep red-brown solution filtered. The filtrate was layered with an equal volume of hexanes. After several days, a black crystalline solid was collected by filtration, washed with hexanes, and dried under vacuum. Yields were typically 20–30%. Some crystals were found large enough for X-ray crystallography. Anal. Calcd for $C_{44}H_{70}N_4S_6V_2$: C, 55.67; H, 7.43; N, 5.90. Found: C, 54.36; H, 7.13; N, 5.70. The product is very air sensitive in both the solid and solution phases.

X-ray Crystallography and Structure Solution. Data were collected on a Picker four-circle diffractometer by using standard low-temperature facilities; details of the diffractometry, low-temperature facilities, and computational procedures employed by the Molecular Structure Center are available elsewhere.[22] Data collection parameters are summarized in Table I. Both structures were solved by MULTAN and Fourier techniques and refined by full-matrix least-squares methods.

For complex **1**, a systematic search of a limited hemisphere of reciprocal space yielded a set of reflections that exhibited $P4/mmm$ diffraction symmetry, indicating a tetragonal unit cell. The observed general conditions for hkl of $l = 2n$ and $0k0$ observed for $k = 2n$ lead to the unique choice of the noncentrosymmetric space group $P\bar{4}2_1c$. A total of 1011 reflections were collected; following the usual data processing, 521 unique reflections remained. Since this is a noncentrosymmetric space group, only one set of each Friedel pair was collected; the R for averaging of 399 redundant (non-Friedel) reflections was 0.049. Of the 521 unique reflections, 483 were considered observed ($F > 3.0\sigma(F)$) and only 16 were

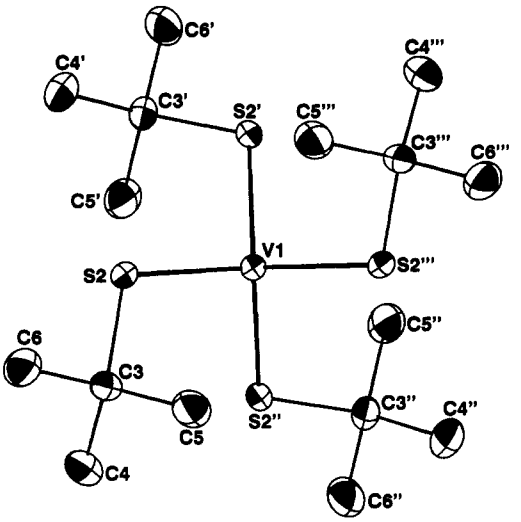

Figure 1. ORTEP representation of complex **1** at the 50% probability level. The view is approximately down the S_4 axis.

equal to 0.0. All non-hydrogen atoms were refined anisotropically; all hydrogen atoms were visible in subsequent difference Fourier maps and included in the final refinement cycles with isotropic thermal parameters. The final difference map was essentially featureless, the largest peak being 1.03 e/Å^3 near the V atom. Since the space group $P\bar{4}2_1c$ is noncentrosymmetric, it was necessary to determine the absolute structure or the "absolute polarity".[23] In this particular space group this means determining the absolute axis assignment for the x and y axes. The assignment opposite to the one given in this report yielded a final R of 0.043, clearly the incorrect assignment.

For complex **2**, a systematic search of a limited hemisphere of reciprocal space yielded a set of reflections that exhibited monoclinic symmetry ($2/m$). The systematic extinction of $0k0$ for $k = 2n + 1$ and of $h0l$ for $h + l = 2n + 1$ uniquely identified the space group as $P2_1/n$. A total of 7761 reflections were collected in the given range. Following data reduction, and averaging of redundant data, a unique set of 5329 reflections were obtained. A total of 2102 reflections having $F > 2.0\sigma(F)$ were considered observed and used for the final refinements. The R for the averaging was 0.07 for 1461 redundant data. All cation and anion non-hydrogen atoms were readily located, but the CH_3 groups on one Bu^t group on V36 were disordered about two positions; these were refined with fixed occupancies of 50%. In addition, a difference Fourier map revealed a disordered solvate molecule, probably hexane or badly disordered THF, and seven peaks were included in refinement cycles, five with occupancies of 100% and two with occupancies of 50%. The solvate atoms are well separated from the metal species and have no importance to the structure of the latter; as such, we did not deem it warranted to pursue a better model for the disorder. Only the V atoms were refined anisotropically, and H atoms were included in fixed calculated positions. The final difference Fourier was essentially featureless, the largest peak being 0.64 e/Å^3 near the disordered solvate molecule.

Mass Spectrometry (MS) Studies. V(SBu^t)$_4$ was examined by electron ionization (EI) MS using a triple quadrupole mass spectrometer (TQMS) in both MS and MS/MS modes. The instrument was built in-house, and complete instrumental details are given elsewhere.[24] Each sample mass was approximately 25 mg and was introduced by a direct insertion probe. The temperature was ramped from room temperature to 150 °C at a 31 °C/min rate. The ion source was set at 70 eV, and the detector was in the positive ion mode. For MS detection, quadrupole 1 was the scanning quadrupole; no collision gas was used in quadrupole 2. For MS/MS detection, the sample was introduced in the same manner. Quadrupole 1 was set at either m/z 407, 408, or 409, and Kr was used as the collision gas in quadrupole 2 to afford collisional activated dissociation (CAD). Quadrupole 3 was the scanning quadrupole.

Other Measurements. Cyclic voltammograms were recorded on an IBM Model EC225 voltammetric analyzer using a standard three-electrode assembly (glassy-carbon working, Pt-wire auxiliary, SCE reference) and 0.1 M $NBu^n_4ClO_4$ as supporting electrolyte. The scan rate was 100 mV/s, and no iR compensation was employed. EPR spectra were recorded on a Bruker ER 300 spectrometer operating at ca. 9.4 GHz

(21) Manzer, S. E. *Inorg. Synth.* **1983**, *21*, 135.
(22) Chisholm, M. H.; Folting, K.; Huffman, J. C.; Kirkpatrick, C. C. *Inorg. Chem.* **1984**, *23*, 1021.
(23) Jones, P. G. *Acta Crystallogr., Sect. A* **1984**, *A40*, 660.
(24) Wong, C. M.; Crawford, R. W.; Barton, V. C.; Brand, H. R.; Neufeld, K. W.; Bowman, J. E. *Rev. Sci. Instrum.* **1983**, *54*, 996.

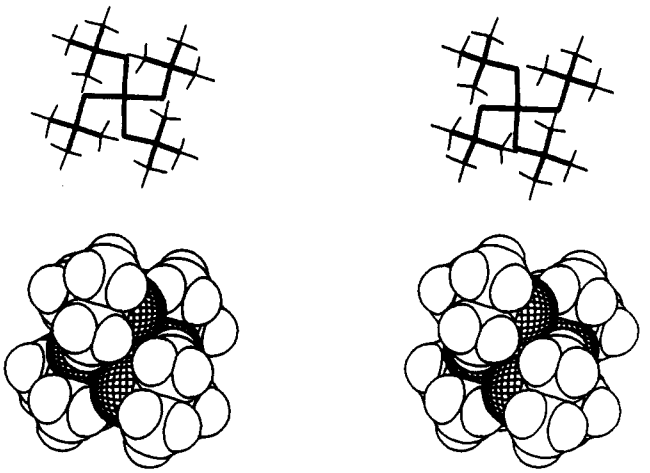

Figure 2. Stereoviews of complex **1**, emphasizing the envelopment of the metal by the hydrophobic ligands.

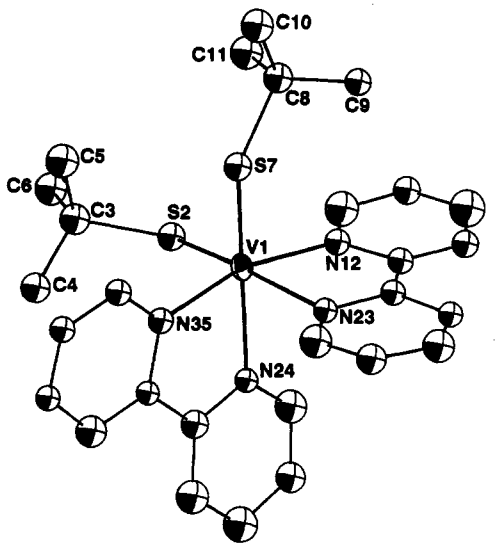

Figure 3. ORTEP representation of the cation of complex **2** at the 50% probability level. Carbon atoms of the bpy ligands are numbered in sequence around the rings.

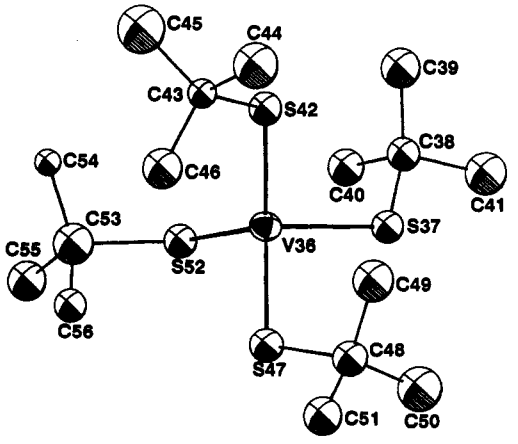

Figure 4. ORTEP representation of the anion of complex **2**.

(X-band); accurate magnetic field values at various spectral positions were obtained with a gaussmeter. The quoted g values include corrections for second-order Zeeman effects.

Results

Procedures have been developed for the synthesis of the complexes $V(SBu^t)_4$ (**1**) and $[V(SBu^t)_2(bpy)_2][V(SBu^t)_4]$ (**2**). Both complexes have been structurally characterized, and the results are presented in Figures 1–4 and Tables I–III. Electrochemical, EPR, and mass spectral studies have been performed on complex **1**, and the results are presented in Figures 5 and 6 and Table IV.

Table II. Selected Fractional Coordinates ($\times 10^4$) and Isotropic Thermal Parameters ($Å^2 \times 10$) for Complexes **1** and **2**

atom	x	y	z	B_{iso}
		Complex **1**		
V1	0	0	10000	15
S2	888 (1)	−1438 (1)	8702 (2)	17
C3	−135 (6)	−2416 (5)	7597 (6)	18
C4	−854 (7)	−3256 (6)	8592 (9)	25
C5	−984 (7)	−1632 (7)	6699 (8)	28
C6	693 (7)	−3172 (8)	6619 (9)	30
		Complex **2**		
V1	9372 (2)	2132 (2)	9907 (2)	16
S2	8927 (3)	806 (4)	9581 (3)	21 (1)
C3	8064 (10)	640 (15)	9590 (13)	25 (5)
S7	8954 (3)	3093 (4)	8970 (3)	21 (1)
C8	9142 (10)	2990 (15)	7926 (12)	24 (5)
N12	10221 (8)	1831 (11)	9390 (10)	18 (4)
N23	10018 (7)	3160 (11)	10304 (9)	16 (4)
N24	9746 (8)	1597 (10)	11034 (9)	15 (4)
N35	8701 (8)	2508 (11)	10703 (10)	18 (4)
V36	8140 (2)	589 (3)	4192 (2)	22
S37	7404 (3)	1274 (4)	3359 (4)	24 (1)
C38	6819 (10)	567 (15)	2800 (12)	25 (5)
S42	7546 (3)	107 (4)	5156 (4)	26 (1)
C43	7903 (10)	−88 (14)	6166 (12)	19 (5)
S47	8870 (3)	1652 (4)	4430 (4)	28 (1)
C48	8552 (11)	2676 (15)	4798 (14)	30 (5)
S52	8590 (3)	−417 (4)	3415 (3)	26 (1)
C53	9232 (12)	−1082 (17)	3952 (15)	38 (6)

Table III. Selected Distances (Å) and Angles (deg)

		Complex **1**	
V1–S2	2.2184 (24)	S2–V1–S2‴	114.45 (12)
S2–V1–S2′	107.04 (6)	V1–S2–C3	116.30 (22)
		Complex **2**	
V1–S2	2.328 (7)	V1–N35	2.127 (16)
V1–S7	2.328 (7)	V36–S37	2.307 (7)
V1–N12	2.123 (17)	V36–S42	2.280 (7)
V1–N23	2.190 (17)	V36–S47	2.290 (7)
V1–N24	2.204 (16)	V36–S52	2.309 (7)
S2–V1–S7	106.0 (3)	N24–V1–N35	76.1 (6)
S2–V1–N12	92.8 (5)	S37–V36–S42	102.3 (3)
S2–V1–N23	164.1 (5)	S37–V36–S47	101.5 (3)
S2–V1–N24	89.5 (5)	S37–V36–S52	104.4 (3)
S2–V1–N35	96.8 (5)	S42–V36–S47	120.9 (3)
S7–V1–N12	98.6 (5)	S42–V36–S52	117.9 (3)
S7–V1–N23	86.9 (5)	S47–V36–S52	106.9 (3)
S7–V1–N25	161.3 (5)	V1–S2–C3	120.5 (8)
S7–V1–N35	91.4 (5)	V1–S7–C8	120.6 (7)
N12–V1–N23	75.9 (6)	V36–S37–C38	116.3 (8)
N12–V1–N24	90.9 (6)	V36–S42–C43	121.0 (7)
N12–V1–N35	163.7 (7)	V36–S47–C48	115.0 (8)
N23–V1–N24	79.8 (6)	V36–S52–C53	113.9 (8)
N23–V1–N35	92.0 (6)		

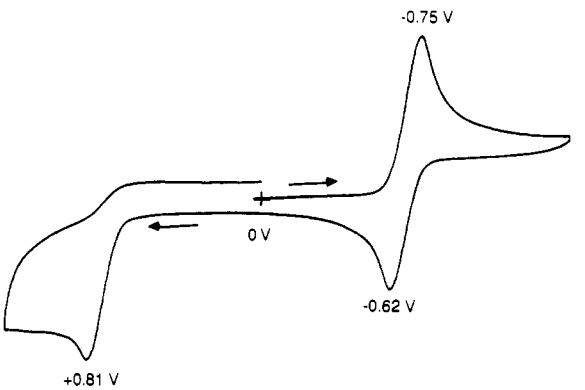

Figure 5. Cyclic voltammogram of complex **1** in CH_2Cl_2 solution at 100 mV/s. Potentials are vs SCE.

Table IV. Relative Intensities[a] of $[VS_xH_y]^+$ Ions Formed in the EIMS of Complex **1**

	y						
x	0	1	2	3	4	5	6
1	54.8	35.1	10.1	nd	nd	nd	nd
2	121.3	72.9	20.9	5.8	nd	nd	nd
3	77.8	126.0	81.4	23.0	8.7	nd	nd
4	43.3	33.5	30.9	151.6	383.4	36.3	6.3

[a] Relative to m/z 51. nd = ion intensity below 0.05% of $C_4H_9^+$.

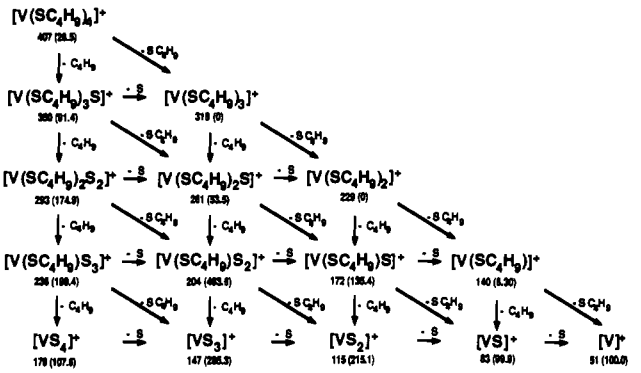

Figure 6. EIMS fragmentation pattern of complex **1**. The m/z value of each ion is indicated; the intensity relative to $[V]^+$ is given in parentheses. The individual fragments represent cluster ions; the indicated intensity is the sum of the individual cluster components.

The results will be detailed in the sections that follow below.

Discussion

Syntheses. Our studies of V/Bu^tS^- chemistry were initiated with the investigation of the reaction between $VCl_3(THF)_3$ and $NaSBu^t$ in MeCN in a 1:3 or 1:4 ratio. Unfortunately, we found it difficult to isolate clean products from these reactions, which yielded both soluble species and intractable dark brown solids. It was noticed, however, that an Et_2O extract of residues remaining after removal of MeCN gave small amounts (typically ~5%) of what proved to be $V(SBu^t)_4$ (**1**), presumably from oxidation of V^{III} by adventitious air or oxidizing impurities in the reagents. Complex **1** had been reported as the product from the reaction of VCl_4 with Bu^tSH/NEt_3;[25] however, the relatively low yield (19%) by the latter procedure, the lack of structural characterization, and our decision to study this molecule in more detail prompted us to seek a convenient and high-yield synthesis and to seek crystals suitable for crystallography. Both objectives were accomplished. Treatment of $VCl_3(THF)_3$ with 3 equiv of $NaSBu^t$ followed by oxidation with Bu^tSSBu^t and minimal workup allows access to high yields of pure product. The synthesis can be summarized in eq 1. A crystallographic investigation (vide infra)

$$VCl_3 + 3NaSBu^t + \tfrac{1}{2}Bu^tSSBu^t \rightarrow V(SBu^t)_4 + 3NaCl \quad (1)$$

confirms complex **1** to be mononuclear as found for $Mo(SBu^t)_4$[26] and $W(SBu^t)_4$[27] and almost certainly the case for $Ti(SBu^t)_4$.[28] The effective magnetic moment in MeCN solution (the Evans method) was found to be 1.75 ± 0.07 μ_B consistent with the V^{IV} (d^1) formulation (spin-only value, 1.73 μ_B). Complex **1** is the only well-characterized example of a homoleptic V^{IV} thiolate, and its mononuclear, four-coordinate nature can be attributed to the steric bulk of the Bu^tS^- group. No doubt other suitably bulky thiolates could also lead to complexes with the $V(SR)_4$ formulation, and obvious examples include arenethiolates with bulky substituents in the 2- and 6-positions, such as was successfully employed[29] for the synthesis of $Mo(TIPT)_4$ (TIPT = 2,4,6-triisopropylbenzenethiolate).

Following our excursion into V^{IV}/SBu^t chemistry, we returned to the VCl_3/Bu^tS^- reaction system. Suspecting that the intractable brown solids might be polymeric in nature ($[V(SBu^t)_3]_n$ and/or $[NaV(SBu^t)_4]_n$) and still desiring to obtain a V^{III}/Bu^tS^- complex, we repeated the $VCl_3/NaSBu^t$ (1:3) reaction in the presence of bpy, aiming for a complex such as $V(SBu^t)_3(bpy)$; the latter would be analogous to $V(TIPT)_3(THF)_2$[30] except for cis rather than trans geometry as a result of the chelating nature of bpy. An extremely air-sensitive product was obtained whose analysis was indeed consistent with the formulation "$V(SBu^t)_3(bpy)$"; however, a subsequent crystallographic investigation showed that a ligand redistribution had occurred and the product to be the salt $[V(SBu^t)_2(bpy)_2][V(SBu^t)_4]$ (**2**) with a six-coordinate cation and four-coordinate anion. The latter is, of course, the one-electron-reduced version of **1**. With hindsight, we believe a contributory factor to the ligand redistribution may be steric pressure in a five-coordinate $V(SBu^t)_3(bpy)$ complex where chelating bpy prevents the Bu^tS^- groups from all occupying preferred equatorial positions of a trigonal bipyramid.

Description of Structures. Complex **1** (Figures 1 and 2) possesses crystallographic $\bar{4}$ (S_4) symmetry, giving only six unique non-hydrogen atoms. The V–S bond lengths are all identical (2.218 (2) Å), and the S–V–S angles are of two types, four of value 107.04 (6)° and two of value 114.45 (12)°; the latter (larger) angles are those bisected by the C_2 (S_4) axis, and this corresponds to a slight flattening of the VS_4 core from T_d to D_{2d} symmetry. The same VS_4 core distortion from T_d to D_{2d} is seen in the isostructural but not isoelectronic (d^2) complexes $M(SBu^t)_4$ (M = Mo^{IV}, W^{IV}),[26,27] where, however, the distortion takes the form of a slightly elongated tetrahedron (four larger and two smaller angles); in addition, the disposition of Bu^t groups is such as to yield overall symmetry of D_2 rather than S_4 as in **1**.

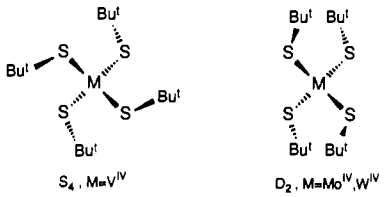

Figure 2 shows stereoviews of the structure including a space-filling diagram; the latter emphasizes the envelopment of V inside a hydrocarbon shell, rationalizing the solubility of **1** in nonpolar solvents such as toluene and hexane.

The structure of complex **2** consists of well-separated $[V(SBu^t)_2(bpy)_2]^+$ cations and $[V(SBu^t)_4]^-$ anions (V···V = 10.255(4) Å). The six-coordinate cation (Figure 3) is the cis isomer and has no imposed symmetry, although it approximates closely to C_2 symmetry, the C_2 axis bisecting the S–V–S angle. The V–N bonds trans to S (2.190 (17), 2.204 (16) Å) are slightly longer than those trans to N (2.123 (17), 2.127 (16) Å), indicating slightly differing trans influences; no noticeable Jahn–Teller distortions are expected for an octahedral d^2 metal. Angular distortions from octahedral geometry are primarily a consequence of the chelating bpy ligands and their restricted bite angles (~76°) and the steric bulk of the cis-Bu^t groups, which opens up the S–V–S angle (106.04 (26)°) and decreases the trans-N23–V1–N24 angle (79.8 (6)°).

The four-coordinate anion of **2** (Figure 4) has no imposed symmetry. The V–S bond lengths are, however, essentially identical (2.280 (7)–2.307 (7) Å) as in **1**, and the S–V–S angles again separate into two larger (117.9 (3), 120.9 (3)°) and four smaller (105.5 (3)–106.9 (3)°) types; the two larger angles (S42–V36–S52 and S42–V36–S47, respectively) are not trans, however, so the distortion of the VS_4 core from T_d cannot be

(25) Preuss, F.; Noichl, H. *Z. Naturforsch.* **1987**, *42B*, 121.
(26) Otsuka, S.; Kamata, M.; Hirotsu, K.; Higuchi, T. *J. Am. Chem. Soc.* **1981**, *103*, 3011.
(27) Listemann, M. L.; Dewan, J. C.; Schrock, R. R. *J. Am. Chem. Soc.* **1985**, *107*, 7207.
(28) Bochmann, M.; Hawkins, I.; Wilson, L. M. *J. Chem. Soc., Chem. Commun.* **1988**, 344.
(29) Roland, E.; Walborsky, E. C.; Dewan, J. C.; Schrock, R. R. *J. Am. Chem. Soc.* **1985**, *107*, 5795.
(30) Randall, C. R.; Armstrong, W. H. *J. Chem. Soc., Chem. Commun.* **1988**, 986.

described as a flattening to D_{2d} as in **1**. On the basis of the variation of S–V–S angles, the best description for the symmetry of the VS_4 core is C_s with the mirror plane defined by S37–V36–S42. The Bu^t groups must not be included for this description to apply; the actual overall symmetry is C_1. Since the anion of **2** is isoelectronic (d^2) with $M(SBu^t)_4$ (M = Mo, W) and, as mentioned above, the latter crystallize with imposed D_{2d} symmetry, it is probably reasonable to conclude that the low symmetry of the anion of **2** is due to crystal packing requirements and forces; the similarly d^2 ($S = 1$) 3d metal complex $Cr(OBu^t)_4$ has been shown to have S_4 symmetry in the gas phase.[31]

In a mixed-complex salt such as **2**, one can always formulate alternative oxidation state assignments, viz. $[V^{II}(SBu^t)_2(bpy)_2][V^{IV}(SBu^t)_4]$ and $[V^{IV}(SBu^t)_2(bpy)_2]^{2+}[V^{II}(SBu^t)_4]^{2-}$; we do not seriously entertain either of these possibilities. The anion V–S distances in **2** (average 2.297 Å) are distinctly longer than those in **1** (2.218 Å), the difference being comparable to that between the covalent radii of six-coordinate V^{IV} and V^{III} (0.06 Å).[32] This is consistent with a one unit lower oxidation level, contrary to both alternative formulations (the difference in covalent radii between six-coordinate V^{IV} and V^{II} is 0.21 Å). In addition, we see no evidence in the cyclic voltammogram (vide infra) of reduction of **1** to the V^{II} level required for the latter alternative, and we strongly suspect that such a formulation would be very unstable to internal electron transfer from the dianion to the dication. We are thus confident of the V^{III} description of **2**.

Electrochemistry and EPR Spectroscopy. With the chemical stability of the $V(SBu^t)_4^{0,-}$ pair established separately in isolated complexes **1** and **2**, an electrochemical study of their interconversion was carried out on complex **1** by using the cyclic voltammetric technique. The results obtained in CH_2Cl_2 solution are shown in Figure 5. As anticipated, complex **1** undergoes a reversible one-electron reduction, at −0.68 V vs SCE; the peak separation at 100 mV/s of 130 mV is comparable with that of the ferrocene/ferrocinium couple under the same experimental conditions (~100 mV). In addition, anodic scans revealed an irreversible one-electron oxidation at a peak potential of +0.81 V and a peak current comparable to those of the reversible couple; these processes define the three-component electron-transfer series in eq 2. The low value of −0.68 V rationalizes the very oxy-

$$V(SBu^t)_4^+ \xleftarrow{+0.81\ V} V(SBu^t)_4 \xrightleftharpoons{-0.68\ V} V(SBu^t)_4^- \qquad (2)$$

gen-sensitive nature of **2**. The irreversible nature of the oxidation process is most probably due to ligand oxidation.

The EPR spectra of complex **1** were recorded at X-band in fluid toluene solution at room temperature (~25 °C) and in a toluene glass at 163 K. The fluid solution spectrum consisted of a typical isotropic signal with the eight-line hyperfine structure characteristic of an interaction between the electron spin and the vanadium nuclear spin (^{51}V, $I = {}^7/_2$). The measured parameters were $g_{iso} = 1.970$ and $A_{iso} = 55$G (51×10^{-4} cm^{-1}). The frozen-glass spectrum displayed axial symmetry consistent with the structure of **1**; the obtained parameters were $g_\parallel = 1.961$, $A_\parallel = 108$ G (99×10^{-4} cm^{-1}), $g_\perp = 1.975$, and $A_\perp = 28$ G (26×10^{-4} cm^{-1}). The distortion of complex **1** from T_d to S_4 symmetry will raise the degeneracy of the e set of orbitals (d_{z^2}, $d_{x^2-y^2}$) containing the unpaired electron; the observed order $g_\perp > g_\parallel$ confirms a $d_{x^2-y^2}$ ground state, since a d_{z^2} ground state would have $g_\parallel > g_\perp$ and a value of $g_\parallel$ close to the free electron value (2.0023).[33] The spectral profiles for **1** are typical of those obtained for numerous vanadyl complexes and, more importantly, for two other four-coordinate non-oxo V^{IV} complexes $V(NEt_2)_4$[34] and $V(OBu^t)_4$.[35] The latter two complexes also have $g_\perp > g_\parallel$ and structures probably also distorted from T_d to S_4 or D_{2d} symmetry although crystallographic data are not available. The most informative further comparison is between complex **1** and $V(OBu^t)_4$, reflecting the S vs O difference. The parameters for $V(OBu^t)_4$ in frozen-CS_2 solution are $g_{iso} = 1.964$, $A_{iso} = 69$ G (64×10^{-4} cm^{-1}), $g_\parallel = 1.940$, $A_\parallel = 138$ G (125×10^{-4} cm^{-1}), $g_\perp = 1.984$, and $A_\perp = 39$ G (36×10^{-4} cm^{-1}). Thus, complex **1** has the larger g_{iso} value and smaller hyperfine coupling constants, consistent with greater covalency in the V–S vs V–O bonds, and a consequent greater delocalization of the electron away from the metal. This is as expected for S vs O if other factors are equal.

Mass Spectrometry of $V(SBu^t)_4$. The most intense ion of the MS analysis of complex **1** was m/z 57, corresponding to the $C_4H_9^+$ alkyl fragment and accounting for 34% of the total ion current. Alkyl fragments $C_3H_6^+$ and $C_2H_5^+$ were also observed with intensities of 50% and 25%, respectively, of the $C_4H_9^+$ ion. Interestingly, methane was observed only at very low concentrations, which is consistent with the fragmentation pattern of the molecule (vide infra). The metal-containing ions were much less intense than the alkyl fragments, with no individual ion being over 5% of the $C_4H_9^+$ fragment intensity. The most intense metal-containing ion was m/z 239, assigned to $[V(SC_4H_9)S_3H_3]^+$. Parent ions with m/z 407, 408, and 409 were detected with similar intensities. This cluster ion behavior is a result of the sample conditions chosen for EIMS as well of the propensity of the compound to undergo self chemical ionization. Given this behavior, the concentration of hydrogen in the ion source can be considered very high.

Figure 6 shows the suggested fragmentation pattern and pathway.[36] As with the parent ion, cluster ions were seen for all the metal-containing fragments. For example, m/z 350 has been assigned to the $[V(SC_4H_9)_3S]^+$ ion. However, also seen is an ion at m/z 351, which is roughly twice as intense and which is assigned as $[V(SC_4H_9)_3SH]^+$. This cluster ion behavior has been seen before in the EIMS of several different types of transition-metal coordination compounds.[37,38]

A prominent feature in Figure 6 (first column) is the stepwise loss of C_4H_9 fragment, producing ions containing progressively more bare S atoms (or SH). This loss of C_4H_9 seems to be a major process, given the high intensity of the resulting fragment ions. This is also supported by $C_4H_9^+$ being the most intense ion in the spectrum. The second column shows the series of fragments related by C_4H_9 loss from the monodeligated $[V(SC_4H_9)_3]^+$ cluster ion. This ion could be formed directly from the parent ion either by loss of SC_4H_9 or stepwise from the loss of a C_4H_9 fragment and then the loss of a S atom. These are likely processes; however, *no* $[V(SC_4H_9)_3]^+$ ions were found in the spectrum. This indicates that either this fragment type is very unstable and immediately fragments further or it is not produced at all. MS/MS results described below indicate the latter because $[V(SC_4H_9)_3]^+$ is produced by CAD. This is further supported by the $SC_4H_9^+$ and $HSC_4H_9^+$ ions having very low intensity, again unlike the case in the CAD fragmentation of $V(SC_4H_9)_4$. Likewise, the $[V(SC_4H_9)_2]^+$ cluster ion is not observed, although the MS/MS results show this ion is produced by CAD. Low-intensity peaks *were* observed at masses m/z 140, 141, and 142, which have been assigned to $[V(SC_4H_9)]^+$. However, the intensities of these peaks were extremely low, and close to noise levels, and are not considered an important species.

The absence of $[V(SC_4H_9)_x]^+$ ($x = 3$–1) and $SC_4H_9^+$ (or $HSC_4H_9^+$) suggests that thiolate loss is not a fragmentation pathway. If we extrapolate further, it also suggests that ions that could have been produced by SC_4H_9 loss have in fact been produced by sequential loss of C_4H_9 and S. There are a variety of fragments of general formula $[V(SC_4H_9)_xS_y]^+$ (x and $y = 1$ or 2) with relatively high intensity. Having ruled out the diagonal

(31) Thaler, E. G.; Rypdal, K.; Haaland, A.; Caulton, K. G. *Inorg. Chem.* **1989**, *28*, 2431.
(32) Shannon, R. D. *Acta Crystallogr., Sect. A* **1976**, *A32*, 751.
(33) Goodman, B. A.; Raynor, J. B. *Adv. Inorg. Chem. Radiochem.* **1970**, *13*, 135.
(34) Holloway, C. E.; Mabbs, F. E.; Smail, W. R. *J. Chem. Soc. A* **1968**, 2980.
(35) Kokoszka, G. F.; Allen, H. C.; Gordon, G. *Inorg. Chem.* **1966**, *5*, 91.
(36) The assignments are strongly suggested but not unequivocally proven by the data. The figure shows only suggested precursors to each fragment; a complete MS/MS analysis is necessary to verify each step.
(37) Reynolds, J. G.; Fish, R. H.; Gallegos, E. J. Manuscript in preparation.
(38) The relationship of these hydrogenated fragments to the corresponding precursor ion cannot be determined without the use of extensive MS/MS detection, which is beyond the scope of this examination.

(SC_4H_9 loss) pathway and remembering that $[V(SC_4H_9)_x]^+$ (x = 1–3) cluster ions are not observed, we can conclude that $[V(SC_4H_9)_2S]^+$, $[V(SC_4H_9)S]^+$, and $[VS]^+$ are probably formed by S loss from the fragment to their left. Note, however, that the three fragments $[V(SC_4H_9)_xS]^+$ (x = 3–1) do not lose S, for this would lead to the unobserved ions $[V(SC_4H_9)_x]^+$ (x = 3–1).

On the basis of the above observations, the following conclusions about the fragmentation of complex **1** can be reached: (i) C_4H_9 fragment loss appears to be a major fragmentation process, contributing to the formation of all ions except where the necessary precursor is not present; (ii) the other major fragmentation process is S loss from ions with more than one bare S atom. Ions with only one bare S atom do not lose this S, with the exception of $[VS]^+$, which gives $[V]^+$. That the source of the S lost is a bare S ligand rather than a thiolate ligand is supported by the complete absence in the spectrum of ions such as $[V(SC_4H_9)_3(C_4H_9)]^+$ (m/z 375, 376, and 377) and $[V(SC_4H_9)_2(C_4H_9)]^+$ (m/z 286, 287, and 288).

The bottom row of Figure 6 shows the intensities and masses of the $[VS_x]^+$ fragments, all with relatively high concentration. Table IV shows the relative intensity of these ions with respect to $[V]^+$. Cluster ions were observed for all values of x ranging from H/S ratios of 0 to >1. This behavior is expected considering the highly electronegative S atoms and the amount of self chemical ionization seen under these conditions. The most intense ion in Table IV is $[VS_4H_4]^+$. This suggests the SH unit is a very stable moiety in the gas-phase chemistry of V–S type compounds in hydrogen-rich environments, a point of relevance to the hydrodemetalation process, as discussed below.

MS/MS Analysis. In order to discern the fragmentation *pathways* of Figure 6, a preliminary MS/MS analysis was carried out on parent ions m/z 407, 408, and 409. This type of analysis uses collisions with uncharged inert gases in quadrupole 2 to generate fragment ions. Because a single ion type can be selected in quadrupole 1 and allowed into the collision cell, this technique is very useful in determining ion–fragment relationships. For parent ion m/z 407, the CAD fragmentation pattern was similar to that shown in Figure 6 except that fragments which would result from loss of whole ligands are observed. $[V(SC_4H_9)_3]^+$ and $[V(SC_4H_9)_2]^+$ cluster ions had intensities of about half that of the parent ion, whereas $[V(SC_4H_9)]^+$ was barely detected. For parent ion m/z 408, only the $[V(SC_4H_9)_3]^+$ cluster ion was observed. The noise was too great in the MS/MS of the m/z 409 parent ion to report data. The detection of these ions in the CAD studies supports the above premise that $[V(SC_4H_9)_x]^+$ ions (x = 3–1) are stable but not formed in the electron ionization of $V(SC_4H_9)_4$. As stated earlier, it further suggests that direct loss of an entire SC_4H_9 ligand is not occurring to any great extent in the fragmentation pattern of Figure 6.

Relevance to the Chemistry of Petroleum Processing. The MS conditions employed in this work are relevant to HDS-type processing conditions. The locally rich hydrogen environment and gas-phase positive ion production of parents and fragments mimic the high H_2 pressure and the gas-phase carbocation chemistry, respectively, found in processes that utilize fluidized- or packed-bed and acid catalysts.

The mechanism by which crude oil vanadium impurities are demetalated and finally deposited on the catalyst has yet to be completely elucidated.[11-14] The currently accepted view, primarily from model compound studies, is that the V-containing compounds are vanadyl (VO^{2+}) species and that they are converted to polymeric vanadium sulfides via a variety of possible intermediates including vanadyl, non-oxo vanadium, "diamagnetic", and VS_x species of various nuclearities.[11,12,39,40]

It is our belief that complex **1** represents a model for some of the non-oxo vanadium intermediates and that its fragmentation behavior can provide insights into the chemistry leading up to V_2S_3 formation. The following scenario can be proposed. Adsorption of vanadyl impurities onto the catalyst is followed by, among other possibilities, loss of the oxygen and some or all of the ancillary ligands. The resulting coordinatively unsaturated metal center now binds the available sulfur ligands in the crude oil (thiolate, sulfide, etc.). The thiolate ligands (and presumably other S-based ligands) are activated to C–S bond cleavage, and alkyl fragments crack from the molecule, leading to mononuclear VS_x species that aggregate to form polynuclear vanadium sulfides and eventually V_2S_3.

The gas-phase behavior of $V(SBu^t)_4$ may also be relevant to other types of petroleum chemistry, for example the formation and mechanisms of function of VS_x slurry catalysts used in entrained flow reactors and for coal liquefaction processes.[41-43] One reasonable possibility is that the S-containing compounds in crude oils react with VS_x to form species similar to $V(SBu^t)_4$ and/or its fragmentation products $V(SBu^t)_xS_y$. The V–S interaction activates the C–S bond, and upon cracking, a higher stoichiometry VS_x is formed. Hydrogen both caps the resulting alkyl group and regenerates the initial VS_x species by forming H_2S. The preparation of these in situ formed slurry VS_x catalysts is usually from oil-soluble vanadyl compound (e.g., $VO(acac)_2$); this conversion may also proceed through $V(SBu^t)_4$-type mechanisms.

Acknowledgment. This work was supported by the Office of Basic Energy Sciences, Division of Chemical Sciences, U.S. Department of Energy, under Grant DE-FG02-87ER13702 (to G.C.). Work at the Lawrence Livermore National Laboratory was performed under the auspices of the U.S. Department of Energy under contract No. W-7405-ENG-48.

Supplementary Material Available: Listings of crystallographic details, atomic coordinates, isotropic and anisotropic thermal parameters, and bond distances and angles (20 pages); listings of observed and calculated structure factors for **1** and **2** (8 pages). Ordering information is given on any current masthead page. Complete MSC structure reports (Nos. 88050 and 89008 for **1** and **2**, respectively) are available on request from the Indiana University Chemistry Library.

(39) Mitchell, P. C. H.; Valero, J. A. *Inorg. Chim. Acta* **1983**, *71*, 179.
(40) Mitchell, P. C. H.; Valero, J. A. *React. Kinet. Catal. Lett.* **1982**, *20*, 219.
(41) Reynolds, J. G.; Yu, S. G.; Lewis, R. T. U.S. Patent 4,559,129, 1985.
(42) Gleim, W. K. T.; Gatsis, J. G. U.S. Patent 3,558,474, 1971.
(43) Boudart, M.; Cusumano, J. A.; Levy, R. B. New Catalytic Materials for Coal Liquefaction. EPRI Report No. RP-415-1; Oct 30, 1975.
(44) *Mass Spectrometry of Metal Compounds*; Charalambous, J., Ed.; Butterworths: London, 1975.